Title

Superior efficacy of a skin-applied microprojection device for delivering a novel Zika DNA vaccine.

Authors

Masavuli, Makutiro

Young, Paul

Gowans, Eric

et al.

Publication Date

2023-12-12

DOI

10.1016/j.omtn.2023.102056

Peer reviewed

Molecular Therapy
Nucleic Acids
Original Article

Superior efficacy of a skin-applied microprojection device for delivering a novel Zika DNA vaccine

Danushka K. Wijesundara,[1,2] Arthur Yeow,[3] Christopher L.D. McMillan,[2] Jovin J.Y. Choo,[2] Aleksandra Todorovic,[2] Zelalem A. Mekonnen,[3] Makutiro G. Masavuli,[3] Paul R. Young,[2] Eric J. Gowans,[3] Branka Grubor-Bauk,[3,4] and David A. Muller[1,2,4]

[1]Vaxxas Biomedical Facility, Hamilton, QLD 4007, Australia; [2]School of Chemistry and Molecular Biosciences, The University of Queensland, Brisbane, QLD 4072, Australia; [3]Discipline of Surgery, The University of Adelaide, Basil Hetzel Institute for Translational Health Research, Adelaide, SA 5005, Australia

Zika virus (ZIKV) infections are spreading silently with limited global surveillance in at least 89 countries and territories. There is a pressing need to develop an effective vaccine suitable for equitable distribution globally. Consequently, we previously developed a proprietary DNA vaccine encoding secreted non-structural protein 1 of ZIKV (pVAX-tpaNS1) to elicit rapid protection in a T cell-dependent manner in mice. In the current study, we evaluated the stability, efficacy, and immunogenicity of delivering this DNA vaccine into the skin using a clinically effective and proprietary high-density microarray patch (HD-MAP). Dry-coating of pVAX-tpaNS1 on the HD-MAP device resulted in no loss of vaccine stability at 40°C storage over the course of 28 days. Vaccination of mice (BALB/c) with the HD-MAP-coated pVAX-tpaNS1 elicited a robust anti-NS1 IgG response in both the cervicovaginal mucosa and systemically and afforded protection against live ZIKV challenge. Furthermore, the vaccination elicited a significantly higher magnitude and broader NS1-specific T helper and cytotoxic T cell response *in vivo* compared with traditional needle and syringe intradermal vaccination. Overall, the study highlights distinctive immunological advantages coupled with an excellent thermostability profile of using the HD-MAP device to deliver a novel ZIKV DNA vaccine.

INTRODUCTION

Zika virus (ZIKV) is a re-emerging flavivirus that is primarily transmitted via the blood meals of a mosquito although sexual and vertical transmission from mother to unborn fetus have been well-documented.[1] It has caused sporadic outbreaks since it was first identified to cause human infections in 1950s.[1] During the 2015–2016 outbreak of ZIKV, millions of people in the Americas were suspected or confirmed to be infected, causing the World Health Organization (WHO) to declare the outbreak a public health emergency. The scale of the outbreak as well as the associated microcephaly with neurological complications in children born to ZIKV-infected mothers, generated worldwide scientific and media attention.

Although the global incidence of ZIKV disease has declined since 2017, WHO has reported 89 countries and territories with evidence of mosquito-borne ZIKV infections. Limited global surveillance suggests that the threat of more ZIKV outbreaks still exists. A recent study suggests that when environmentally relevant selective pressures are applied, novel variants can emerge including those with even a single mutation (I39T) to support an increase in transmissibility and virulence.[2] Furthermore, a mathematical modeling study highlighted that sexual transmission of ZIKV is a significant driver of the ZIKV epidemic.[3] In 18 independent studies reporting sexually acquired ZIKV and 21 studies describing ZIKV in genital fluids, 96.2% of the cases resulted from sexual transmission due to unprotected vaginal exposure to the virus.[4] These findings have prompted WHO to issue recommendations for safer sex practices and abstinence (for at least 6 months) upon return from ZIKV endemic regions to minimize potential risk from the severe damage that ZIKV could cause to the developing fetus during pregnancy.[5] Given that infections are mostly subclinical and result in mild flu-like symptoms, it is highly unlikely that antiviral agents will be useful for treatment of individuals traveling from endemic regions and to prevent the occurrence of an outbreak. Thus, it is important to continue ZIKV vaccine development for emergency use in the likely event of another outbreak occurring in the future.

The ZIKV genome encodes three structural proteins important for cell entry including premembrane (prM) and envelope (E) and seven non-structural proteins important for viral replication, pathogenesis,

Received 9 August 2023; accepted 11 October 2023;
https://doi.org/10.1016/j.omtn.2023.102056.

[4]These authors contributed equally

Correspondence: Danushka K. Wijesundara, Vaxxas Biomedical Facility, Hamilton, QLD 4007, Australia.
E-mail: d.wijesundara@uq.edu.au
Correspondence: Branka Grubor-Bauk, Discipline of Surgery, The University of Adelaide, Basil Hetzel Institute for Translational Health Research, Adelaide, SA 5005, Australia.
E-mail: branka.grubor@adelaide.edu.au
Correspondence: David A. Muller, Vaxxas Biomedical Facility, Hamilton, QLD 4007, Australia.
E-mail: d.muller4@uq.edu.au

and immune evasion.[6] The vast majority of vaccine development efforts since the emergence of the 2015 epidemic have focused on targeting prM and E with efficacy data supporting significant protective effects of induced neutralizing antibodies in small animal models (e.g., mice) and non-human primates.[7] However, antibodies against the virion surface E protein have been reported to potentially enhance infection of dengue virus and vice versa in countries where these viruses co-circulate.[8–10] In contrast, NS1 is a non-structural viral protein, and hence antibodies to the NS1 protein do not cause antibody-dependent infection enhancement (ADE) of flaviviruses.[11] There is also a high degree (99.3%) of homology for the NS1 gene among all ZIKV isolates and so the antibodies elicited are likely to be broadly reactive.[12] Furthermore, the flavivirus NS1 protein has long been recognized as a potent immunogen with the ability to elicit robust humoral and T cell immunity.[13]

DNA vaccines are inexpensive, easy to construct, stable at room temperature, and have minimum side effects, which simplifies handling and distribution suggesting the potential for equitable global distribution of this type of vaccine.[14] DNA vaccines have been shown to be clinically effective. Seminal studies have described histological regression and/or elimination of persistent human papillomavirus (HPV) infection and HPV-related cervical lesions with therapeutic DNA vaccines encoding the HPV E6 and E7 proteins delivered by intramuscular injection and electroporation in humans.[15,16]

During the early stages of the 2015–2016 epidemic, DNA vaccines that elicited protective neutralizing antibodies to ZIKV in mice,[17] and rhesus macaques,[18] were developed. We pioneered a proprietary DNA vaccine (pVAX-tpaNS1) encoding codon-optimized NS1 protein from the Brazilian strain of ZIKV with a tissue plasminogen activator signal sequence to facilitate effective NS1 secretion.[19] Mice vaccinated with pVAX-tpaNS1 controlled the infection after challenge with 200 plaque-forming units (PFU) of ZIKV, as determined by qRT-PCR analysis.[19] The protection was dependent on T cell immunity, with $CD8^+$ cytotoxic T lymphocytes (CTL) facilitating early control of the virus and both $CD4^+$ T helper (Th) cell and $CD8^+$ T cells acting synergistically to provide protection during later stages of infection in immunocompetent wild-type BALB/c mice.

The potential of DNA vaccines is still not fully realized due to poor delivery and antigen expression, and the lack of a localized inflammatory response, essential for antigen presentation and the induction of an effective immunity. There are significant benefits for delivering DNA vaccines into the dermal layers of the skin given the high density of antigen-presenting cells present in the skin, especially in the dermis, compared with other tissues,[20] Furthermore, intradermal (ID) delivery of vaccine antigens can elicit higher magnitude immune responses compared with intramuscular delivery.[14]

The high-density microarray patch (HD-MAP) vaccine delivery technology has been exploited in numerous pre-clinical and clinical protein vaccine studies to demonstrate that it is safe and can elicit potent immune responses in a dose-sparing manner.[21–23] Vaccines are coated on the HD-MAP microprojections and delivered primarily into the upper dermis and partially into the epidermis.[21] Efficacy outcomes of the ZIKV pVAX-tpaNS1 vaccine following ID delivery of the vaccine were described previously.[19] In the current study, we investigated whether pVAX-tpaNS1 delivered using Vaxxas's HD-MAP technology can elicit more potent NS1-specific immunity *in vivo* and protection against ZIKV compared with typical needle and syringe ID vaccination. Our findings showed that HD-MAP delivery of pVAX-tpaNS1 vaccine afforded mice protection against live ZIKV challenge, elicited cervicovaginal immunity, and significantly enhanced the magnitude and breadth of Th cell and CTL responses *in vivo* compared with ID vaccination. This is the first study to demonstrate this effect *in vivo* in the context of DNA vaccination against flaviviruses using a microneedle delivery device and delineates a distinctive, immunological advantage of using the HD-MAP technology to deliver nucleic acid vaccines.

RESULTS

Endotoxin-free pVAX and pVAX-tpaNS1 DNA plasmids were validated prior to vaccination studies with restriction enzyme digests, agarose gel electrophoresis. Effective antigen expression of NS1 was confirmed by immunofluorescence in transfected HEK293T cells. Linearization of DNA vaccines with HindIII and analysis on agarose gel electrophoresis confirmed the expected size (Figure 1A) of pVAX to be ~3 kb and pVAX-tpaNS1 to be ~4.1 kb (Figure S1A). NS1 expression was confirmed in pVAX-tpaNS1 transfected HEK293T cells, by immunofluorescence, but not in pVAX transfected HEK293T cells (Figure S1B).

Thermostability is an important feature of any vaccine especially for large-scale distribution in low- to middle-income countries that suffer from lack of access to adequate cold-chain distribution and storage. Consequently, we performed thermostability analysis of validated pVAX-tpaNS1 at room temperature (RT) (20°C–25°C) and at 40°C for 4 weeks following coating of 25 μg of the DNA vaccine on HD-MAP in 1% methylcellulose. Liquid controls (LCs) consisting of the DNA formulation used for coating HD-MAP were subjected to the same analysis to determine whether dry-coating on HD-MAP offered an advantage. We quantified pVAX-tpaNS1 eluted from HD-MAP immediately after coating (D0) as well as 14 and 28 days later using PicoGreen assay. Recovered DNA was characterized for plasmid integrity with agarose gel electrophoresis (Figures 1B and 1C). NS1 antigen expression was evaluated using immunofluorescence analysis (Figure 1D). Gel electrophoresis analysis of DNA eluted immediately after coating (i.e., D0) suggested that drying onto the surface of HD-MAP did not result in any degradation of the DNA, although more circular forms of the DNA were obvious relative to the LC (Figure 1B). Linearization of the eluted plasmid at D0 with HindIII resulted in a single band at the expected size of ~4.1 kb which further supports the maintenance of the plasmid integrity when coated on the patch using 1% methylcellulose (Figure 1B). The same trend supporting plasmid stability on the patch was observed for eluted patch samples stored for 14 and 28 days at RT and 40°C despite the conformation of the plasmid existing mostly in the circular form at 40°C for all samples tested including the LCs (Figure 1B). Importantly, comparable amount of DNA was recovered following elution of coated

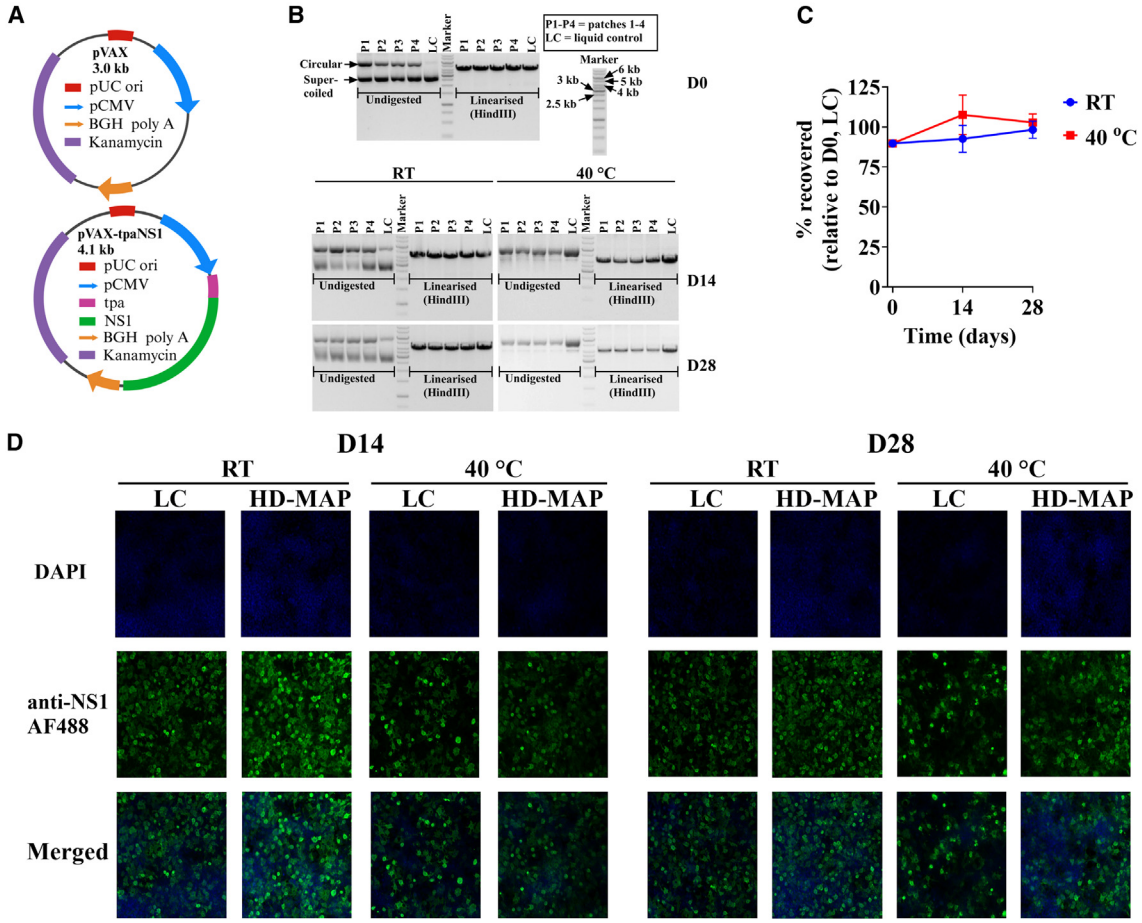

Figure 1. Thermostability of pVAX-tpaNS1 following coating on the HD-MAP

(A) Plasmid map and the theoretical size of pVAX and pVAX-tpaNS1. (B) Agarose gel electrophoresis analysis of pVAX-tpaNS1 eluted immediately after coating (D0) or eluted following 14 (D14) and 28 (D28) days of storage at RT or 40°C in a dry-coated state on the HD-MAP. Data from four patches (P1-P4) and the liquid control (LC) are shown; 25 μg of DNA in 21 μL of the formulation cocktail was used to coat each patch. (C) The amount of DNA recovered from eluted patches over time for the stability study in (B) relative to the LC at D0. Data from four patches per time point are shown and the error bars depict the standard deviation. (D) Immunofluorescence analysis of samples for the study described in (B). A representative image of the LC and a patch (HD-MAP) incubate for 14 and 28 days at RT or 40° C are shown. Merged images are a combination of the respective DAPI and AF488 conjugated ZIKV anti-NS1 stained images.

patches at RT and 40°C irrespective of the time point analyzed (Figure 1C). Furthermore, immunofluorescence analysis of transfected HEK293T cells showed no difference in NS1 expression from pVAX-tpaNS1 recovered from HD-MAP or LCs after 14 or 28 days of storage at RT or 40°C (Figure 1D). Overall, we demonstrated that coating of pVAX-tpaNS1 on HD-MAP imparted comparable thermostability relative to liquid storage and was effective in maintaining the integrity and expression capacity of pVAX-tpaNS1 in the dry-coated state.

We next evaluated the protective efficacy of pVAX-tpaNS1 delivered via ID or the HD-MAP in a prime-boost regimen shown in Figure 2A. BALB/c mice were prime-boost vaccinated with 5, 25 or 50 μg of pVAX-tpaNS1 or placebo (50 μg of pVAX) prior to the intravenous challenge with 200 PFU of ZIKV PRVABC59 strain and viral load analysis 1 day post-challenge (Figure 2A). All of the pVAX-tpaNS1 vaccinated groups were able to restrict ZIKV infection relative to the respective placebo control (pVAX), although this trend was not statistically significant in the 5 μg HD-MAP group (Figure 2B). In the HD-MAP group there was a clear dose-dependent reduction in the viral load with the higher doses favoring increased control of viremia which was not observed in the ID group (Figure 2B). When comparing vaccine dose-matched, mean viral load between ID and HD-MAP cohorts, only the 5 μg ID group had a statistically significant reduction in viremia relative to the respective HD-MAP group (Figure 2C). However, the mean viral load and the standard deviation were the lowest in the 50-μg HD-MAP dose among all the pVAX-tpaNS1 vaccination groups, which suggests that the 50-μg HD-MAP dosing regimen elicited the most reproducible and robust level of protection (Figure 2C).

We next investigated whether 50 μg HD-MAP dosing regimen elicits more robust humoral and/or T cell-mediated immunity compared

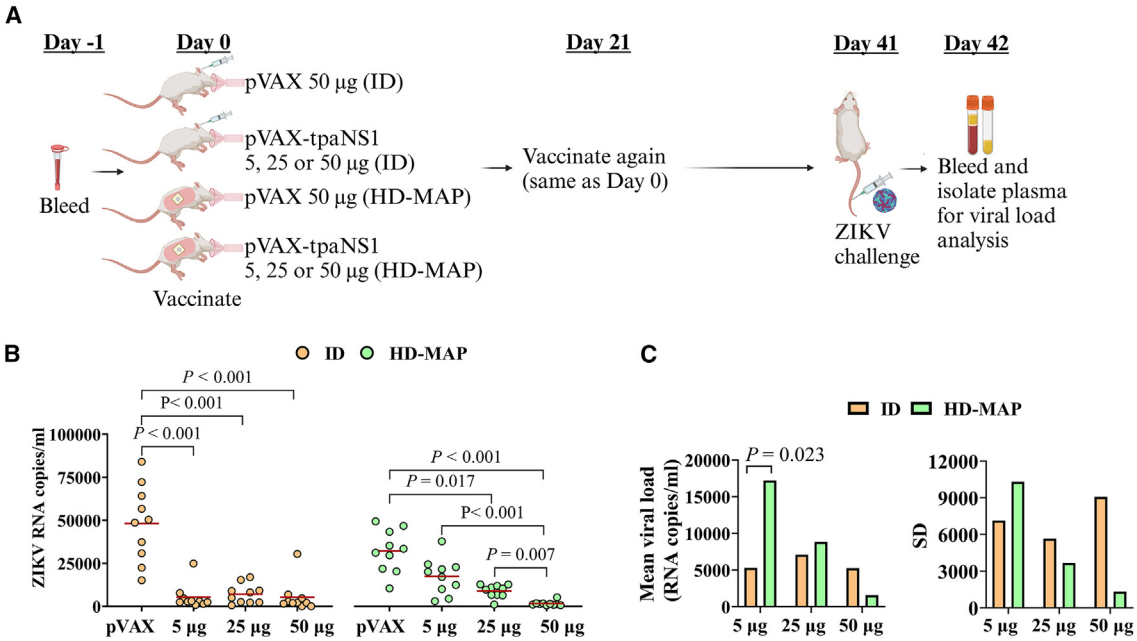

Figure 2. HD-MAP vaccination with pVAX-tpaNS1 elicits reproducible protection in a dose-dependent manner

(A) Study schedule (n = 10 per group). (B) Viral load as measured using RT-PCR for ZIKV RNA copies/mL 1 day post-challenge with 200 PFU of ZIKV for the mice in (A). Values that were below 100 copies/mL were plotted as 50 copies/mL or half the limit of detection. (C) Mean viral load and standard deviation (SD) for the analysis in (B). p values were generated using a pairwise Kruskal-Wallis test using IBM SPSS Statistics Software (Version 29) and only shown for comparisons that reached statistical significance ($p < 0.05$).

with the respective ID vaccination with pVAX-tpaNS1 (Figure 3A). BALB/C mice were vaccinated in a prime-boost manner and serum anti-NS1 immunoglobulin (Ig)G titers were measured a day prior to each vaccination (day −1 and day 20) as well as 15 (day 35) and 21 days (day 42) after the boost. Furthermore, we evaluated if HD-MAP vaccination induced mucosal IgG and IgA 21 days after boost by analysis of titers in vaginal lavage of vaccinated animals (Figure 3B). When comparing the serum IgG endpoint titers following the prime (day 20) and booster (day 35 and day 42) vaccinations, the responses were nearly identical between the HD-MAP and ID groups (Figure 3C). Furthermore, HD-MAP and ID vaccination regimens reproducibly elicited similar levels of cervicovaginal IgG titers, but not IgA titers (Figure 3B). Overall, the data suggest that the mucosal and systemic antibody response elicited following HD-MAP and ID vaccination with the 50-µg pVAX-tpaNS1 dosing regimens were comparable. Nonetheless, the vaccine is known to elicit protection in a T cell-dependent manner, which we explored *in vivo* in the same vaccination study (Figure 3A) using an established fluorescent target array (FTA) analysis.[19]

The FTA preparation involves labeling of naive autologous splenocytes with a combination of titrated concentrations of cell tracking dyes resulting in unique fluorescent bar-coded cell populations. For the FTA preparation of the vaccination study (Figure 3A), we labeled naive autologous splenocytes with cell trace violet (CTV) and cell proliferation dye efluor670 (CPD) (Figure 4A). The fluorescent bar-coded cells were pulsed with major histocompatibility (MHC) class I and II binding peptides for intravenous challenge. In the current study, we pulsed targets with four peptide pools (P1-P4), which collectively span the vaccine-encoded ZIKV NS1 protein and also incorporated immunodominant peptides for CTL (peptides 87 and 88) and Th cell (peptides 68 and 69) responses that we have mapped previously[19] (Figure 4A). CTL responses are detectable when the pulsed targets are killed relative to unpulsed, "nil," control. Th cell responses can be detected when the bar-coded naive B cells ($B220^+$) in the FTA present cognate peptide-MHC-class II complexes to Th cells that provide costimulation resulting in the activation and up-regulation of the activation marker, cluster of differentiation 69 (CD69), on the cell surface of cognate-peptide-presenting B cells (Figures 3A and 4A).

HD-MAP pVAX-tpaNS1 vaccination was superior and elicited significantly higher Th cell and CTL responses to all NS1 peptide pulsed targets with the exception of P1 and P4 in the case of Th cell response relative to the respective placebo control (Figures 4B and 4C). Consistent with our previous study,[19] pVAX-tpaNS1 vaccination elicited dominant CTL response to NS1 P4 and immunodominant peptides 87 and 88 and dominant Th cell response to NS1 P3 and peptides 68 and 69 (Figures 4B and 4C). When comparing ID versus HD-MAP vaccination with pVAX-tpaNS1, the HD-MAP group exhibited significantly higher magnitude of CTL response to P2, P3, P4, 68, 69, 87, and 88 peptide pulsed FTA cells (Figure 4B). The same trend was represented in the Th cell response, although there were no statistically significant

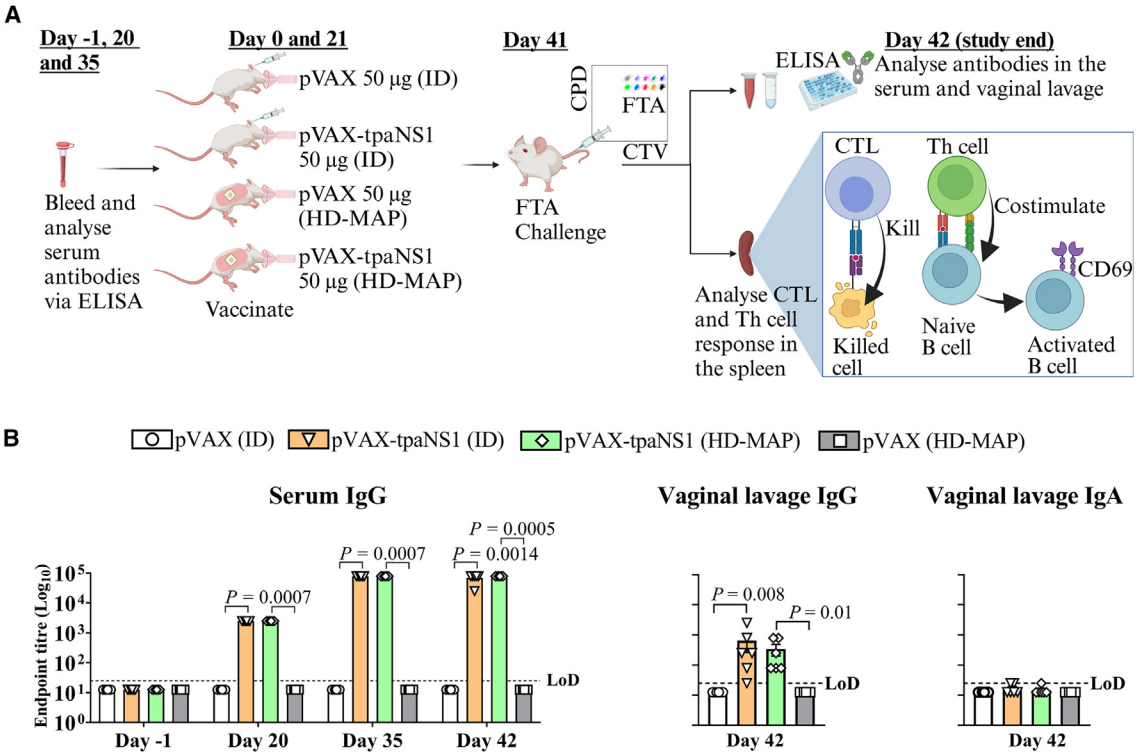

Figure 3. HD-MAP with pVAX-tpaNS1 elicits cervicovaginal IgG immunity and superior systemic IgG response compared with the respective ID vaccination

(A) Study schedule (n = 6 per group). (B) Serum anti-NS1 IgG endpoint titers for the bleeds performed in the study and cervicovaginal lavage anti-NS1 IgG and IgA titers at the end of the study shown in (A). p values are shown for comparisons that reached statistical significance ($p < 0.05$) and values that were below the limit of detection (LoD) were simply annotated as $^1/_2$ the reciprocal of the LoD. p values were generated using a pairwise Kruskal-Wallis test in GraphPad Prism version 9.0. Error bars depict the standard error of the mean.

differences for P4 and responses to peptide 87, which is unsurprising as both are immunodominant for CTL and not Th cell responses (Figure 4C). Importantly, vaccination with HD-MAP resulted in increased breadth of NS1-specific CTL and Th cell responses to target P2 in the HD-MAP pVAX-tpaNS1 vaccination group, which was not observed for the ID group here or in our previous study[19] (Figures 4B and 4C). Overall, HD-MAP vaccination elicited enhanced T cell responses, as measured by significant increase in breadth and magnitude of NS1-specific Th cell and CTL responses *in vivo*.

DISCUSSION

We report superior *in vivo* immunogenicity and protective efficacy of a novel DNA vaccine targeting ZIKV NS1 when delivered into the dermis using a microarray patch, HD-MAP. The data showed that HD-MAP delivery of the vaccine elicited more reproducible protection in immunocompetent mice in a dose-dependent manner. HD-MAP protective response was characterized by more potent and broader T cell responses *in vivo* compared with traditional needle-based delivery of the vaccine. Importantly, HD-MAP-coated pVAX-tpaNS1 was stable at ambient temperature in the laboratory (i.e., 20°C–25°C) and at 40°C with no significant loss in the integrity or expression capacity of the recovered DNA following storage over the course of 4 weeks. Despite the many benefits of using DNA vaccines, it is widely appreciated that a delivery device is required for DNA vaccines to be effectively delivered and/or to overcome poor immunogenicity. The current study highlights that the HD-MAP device can facilitate long-term storage of DNA vaccines such as pVAX-tpaNS1 in a dry-coated state and improve the immunogenicity of pVAX-tpaNS1 when used for vaccine delivery. Stability at RT and high temperatures removes the need for cold-chain storage and distribution methods associated with both traditional and mRNA vaccines, thus reducing the costs of deployment and likely broader distribution. These features are particularly desirable for successful deployment of DNA vaccines for emergency use to benefit low- to middle-income countries.

We have shown that secretion of NS1 following vaccination with pVAX-tpaNS1 elicits a rapid immune response that provides protection in immunocompetent mice in a $CD8^+$ T cell-dependent manner with accompanying $CD4^+$ Th cell responses contributing to protection.[19] Since our publication, a number of candidate vaccines targeting ZIKV NS3 using DNA or RNA platforms have elicited potent CTL immunity, which was necessary for protection of pregnant mice and their fetuses.[24,25] These findings provide further support that non-structural proteins of ZIKV can elicit potent, protective CTL immunity. There is

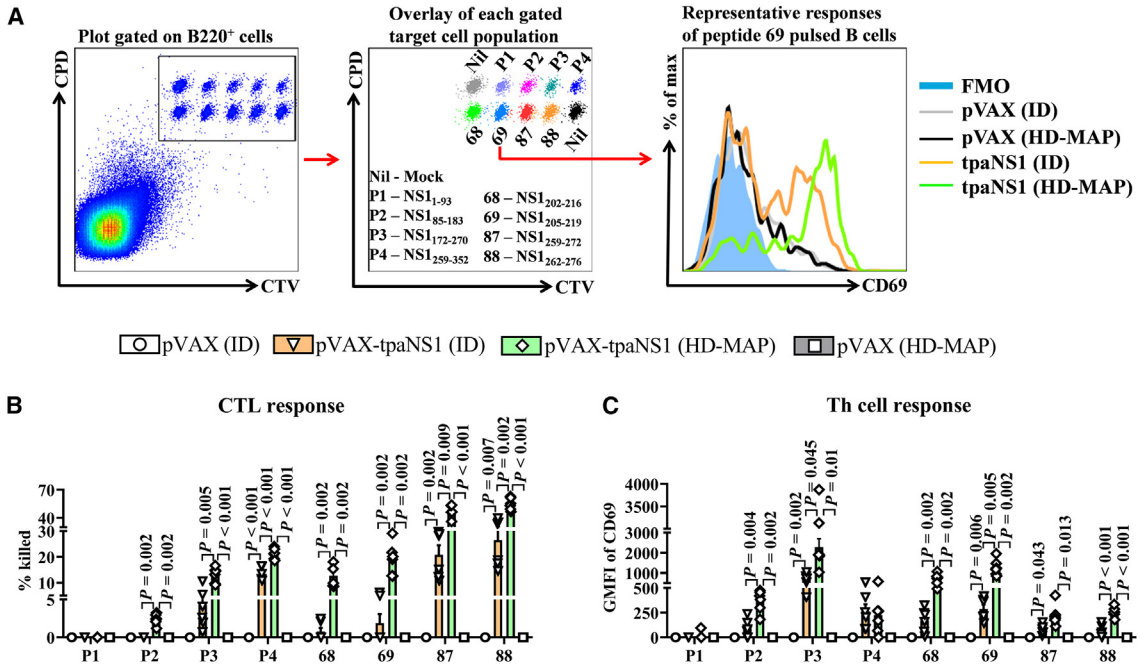

Figure 4. Superior NS1-specific Th cell and CTL response of HD-MAP-based pVAX-tpaNS1 vaccinated mice

(A) Mice were vaccinated and FTA challenge performed exactly as shown in Figure 3A. Representative flow cytometry plots of splenocytes 18 h post FTA challenge delineating the Th cell response analysis are shown. The dot plots show the gating of FTA cells recovered from a pVAX (ID) group and the overlay of each gated target cell population pulsed with the indicated peptide pools or mock (nil). The histogram plot shows a representative response from each group and depicts the expression of CD69 on peptide 69-pulsed B cells. (B and C) CTL (B) and Th cell (C) response to NS1-peptide pulsed targets. p values are shown for comparisons that have yielded statistically significant results (i.e., $p < 0.05$) when evaluated using a Welch's ANOVA with Games-Howell post hoc test. IBM SPSS Statistics Software (Version 29) was used to calculate the p values. Error bars depict the standard error of the mean.

empirical evidence to suggest that T cell responses that target multiple epitopes of non-structural proteins could boost cross-reactive T cell immunity to conserved immunogenic regions shared with other flaviviruses such as DENV to facilitate cross-protection.[26] HD-MAP-based delivery of pVAX-tpaNS1 elicited CTL and Th cell responses, which targeted $NS1_{85-352}$ including immunodominant Th cell epitopes in the $NS1_{202-219}$ region and immunodominant CTL epitopes in the $NS1_{259-272}$ region. The $NS1_{85-352}$ also comprise several immunodominant T cell epitopes predicted to be immunogenic in humans and cross-reactive with viruses in the Flaviviridae family.[12,27] Thus, there is potential for the pVAX-tpaNS1 vaccine especially when used with the HD-MAP to elicit broadly cross-reactive and cross-protective flavivirus T cell immunity.

The conformational similarities of NS1 from ZIKV, DENV, and West Nile virus,[28] and the ability of NS1-specific monoclonal antibodies to elicit cross-protection against these viruses,[29,30] in the absence of ADE are attractive features for its use to elicit antibody-mediated protection. pVAX-tpaNS1 HD-MAP vaccination elicited robust serum anti-NS1 IgG response, which was also detected in the cervicovaginal mucosa albeit at lower titers. A recent study from Wessel et al.,[31] showed that monoclonal antibodies targeting ZIKV NS1 are protective during pregnancy, adding to the promise of targeting NS1 via pVAX-tpaNS1 HD-MAP vaccination.

We have previously shown that effective secretion was crucial for eliciting NS1-specific antiviral cytokine secreting and polyfunctional T cell responses following *in vitro* peptide stimulation, which correlated with *in vivo* T cell responses as evaluated using the FTA assay.[19] In the current study, we used the high-throughput FTA assay to obtain a real-time snapshot of the magnitude and breadth of the Th cell and CTL immunity *in vivo* obviating the need to perform prolonged peptide stimulation of T cells *in vitro* as is the case with classical T cell functional assays. Furthermore, Th cell responses are important for maturation of antibody-producing B cell responses and in this regard the FTA assay is uniquely valuable because it measures the ability of vaccine-elicited $CD4^+$ Th cells to activate cognate-peptide-presenting B cells.[32] The current study, to our understanding, is the first to demonstrate that a microneedle device was able to elicit strong antibody responses along with Th cell and CTL responses *in vivo* in the context of flavivirus vaccinations. Specifically, we showed that HD-MAP vaccination elicited a higher magnitude and broader response compared with ID vaccination with the response broadening to target ZIKV $NS1_{85-183}$ (P2), a region that has not been characterized to be a T cell immunogen in previous studies.[19,33,34]

Consistent with our previous study,[19] ID vaccination with pVAX-tpaNS1 elicited Th cell responses in the absence of CTL immunity to $NS1_{202-219}$ (peptides 68 and 69). Intriguingly, HD-MAP vaccination

with pVAX-tpaNS1 elicited robust Th cell and CTL immunity to $NS1_{202-219}$. CTLs are typically $CD8^+$ T cells, but this observation allows us to speculate that HD-MAP relative to ID vaccination with pVAX-tpaNS1 enhances the plasticity of vaccine-specific $CD4^+$ T cells such that helper and cytotoxic functions are uniquely acquired. This is likely given that $CD4^+$ CTL exhibit a transcriptome and cytokine production profile typically found in Th cells.[35]

Among T cells, $CD4^+$ population is characterized to have the greatest number of subsets and yet there are no markers to categorize $CD4^+$ CTL as a distinct subset, although at least one study has highlighted that class-I restricted T cell-associated molecule is a potential candidate for this purpose.[35,36] The ontogeny of $CD4^+$ CTL is unclear, but it is appreciated that they are mostly derived from $CD4^+$ T cells that have acquired a Th1 phenotype or produced interferon (IFN)-γ and interleukin (IL)-2. It is well-established that plasmid DNA molecules, owing to the presence of unmethylated CpG motifs, have the capacity to activate the toll-like receptor 9 pathway to promote the development of Th1 and CTL responses.[37,38] We have previously shown that ID vaccination with pVAX-tpaNS1 elicited a robust Th1 response involving the production IFN-γ and IL-2,[19] despite ID vaccination not supporting the development of a CTL response to an immunodominant Th cell epitope (i.e., $NS1_{202-219}$). Thus, future studies should investigate whether potentially elevated levels of antigen presentation or heightened Th1 responses resulting from HD-MAP vaccination with pVAX-tpaNS1 directly impact the development of $CD4^+$ CTL against $NS1_{202-219}$. In this regard, the vaccination module in the current study could represent a unique *in vivo* model to further investigate aspects related to the ontogeny and significance of $CD4^+$ CTL as well as cellular markers to delineate this subset to benefit future studies.

NS1 is a highly conserved protein among flaviviruses and secreted during pathogenic flavivirus infections. Consequently, it is possible to adapt the pVAX-tpaNS1 vaccination strategy on a virus-by-virus or as a vaccine cocktail to target flaviviruses in general. In this regard, HD-MAP-based delivery of the vaccine(s) could increase the breadth of immunity and protection. The scale-up, distribution, and ease of distribution capacities of pVAX-tpaNS1 as a dry-coated vaccine on the HD-MAP are not expected to pose significant issues for equitable distribution owing to the following reasons: (1) thermostable and cost-effective nature of producing pVAX-tpaNS1/HD-MAP using only 1% methylcellulose for dry-coating purposes in the absence of any adjuvants, and (2) Vaxxas Pty. Ltd. have developed the manufacturing capacity to aseptically scale-up the HD-MAP production and a simple "click"-based HD-MAP application system for self-use in the absence of specialized health or vaccine administration professionals. However, in endemic regions, pre-existing immunity to flaviviruses is common. This will cause person-to-person variations in the immunodominance hierarchy and the pre-existing pool of effector/memory NS1-specific B and T cell clones that can be protective or pathogenic. Given the lack of vaccine efficacy trials for ZIKV in humans, it remains yet to be determined whether any vaccination, including vaccination against NS1, can boost pre-existing immunity and elicit *de novo* immune responses that are protective rather than pathogenic. This is a caveat of the pVAX-tpaNS1 vaccination approach that can only be addressed in human clinical trials prospectively.

It will be of interest to determine whether the pVAX-tpaNS1 vaccination strategy can be adapted for use with encapsulated mRNA given the recent success of this platform against severe acute respiratory syndrome coronavirus 2 on a global scale. Although unlikely to be more stable and cost-effective to manufacture than DNA, it is possible that encapsulated mRNA will enhance the uptake of the vaccine at the vaccination site resulting in more robust and protective immunity compared with DNA.

In conclusion, we highlight the potential of using the HD-MAP technology to deliver DNA vaccines to elicit robust IgG, Th cell, and CTL responses including mucosal responses *in vivo* that can serve beneficial roles for protection against sexual transmission of ZIKV. Additionally, the study highlights that HD-MAP vaccination can broaden T cell immunity and potentially activate atypical immune pathways, not known to be elicited for other flavivirus vaccines, to facilitate the development of $CD4^+$ CTL. These immune features are desirable for vaccination strategies designed to target rapidly mutating intracellular pathogens such as RNA viruses and even cancer immunity.

MATERIALS AND METHODS

DNA constructs, HD-MAP, and immunizations

NS1 from Brazil-ZKV2015 isolate was cloned downstream of the cytomegalovirus promoter and a Kozak translation initiation sequence encoded in the pVAX plasmid (Life Technologies) as previously described.[19] Endotoxin-free pVAX and pVAX-tpaNS1 DNA plasmids were prepared using QIAGEN endotoxin-free Gigaprep kits. Prior to all animal studies, plasmid integrity was analyzed on 0.8% agarose gel electrophoresis in the presence or absence of HindIII enzyme digestion, which was performed according to manufacturer's recommendations (New England Biolabs).

Patches (HD-MAP) were a gift from Vaxxas Pty. Ltd. and produced following injection molding of medical-grade synthetic polymer to produce 5,000 microprojections/cm^2 with each projection being 250 μm in length. For coating DNA on the HD-MAP, DNA was formulated in 1% methylcellulose and ultrapure water (Thermofisher Scientific) and 21 μL of the formulation was applied to each patch that has previously been treated with an oxygen plasma cleaner to facilitate dry-coating of coating solutions, as we have previously described.[39] Coating formulation was dried on the patches using a sterile-filtered nitrogen gas stream as previously described.[40] For immunizations with the HD-MAP, DNA-coated patches were applied to the skin flank of mice following shaving and depilatory cream application as we have previously described.[39] ID immunizations were performed with excipient-matched vaccine formulations relative to the HD-MAP coating solution and delivered to the ear pinnae as we have previously described.[19]

Mice

Age-matched 6- to 8-week-old female BALB/c mice were purchased from the Monash University and allowed to acclimatize for at least

5 days prior to experimental use at the University of Queensland Biological Resources Facility and The University of Adelaide. Mice were housed in individually ventilated cages and all procedures performed were conducted in accordance with the ethical oversight of the University of Queensland's Animal Ethics Committee protocol 2021/AE000340 and the University of Adelaide Animal Ethics Committee protocol M-2021-080.

Immunofluorescence for NS1 expression

For analysis of NS1 expression, 200 ng of pVAX-tpaNS1 or pVAX formulated with Lipofectamine LTX reagent in accordance with the manufacturer's protocol (Life Technologies) was used to facilitate transfection of 70%–90% confluent HEK293T cell cultures seeded in 96-well plates. Forty-eight hours post-transfection, adherent HEK293T cells were fixed with 4% formalin, permeabilized with methanol, and incubated with 1:200 diluted pooled anti-NS1 mouse sera for 2 h at 37°C as we have described.[19] Then, 1:300 diluted Alexa Fluor 488 (AF488) conjugated goat anti-mouse IgG (ThermoFisher Scientific) was added and incubated for further 2 h prior to performing an additional staining step with 300 nM 4′,6′-diamidino-2-phenylindole (DAPI, Life Technologies) for 5 min at RT as described.[19] The stained cells were visualized using the Zeiss LSM-700 microscope and representative images analyzed using Zeiss's Zen software.

PicoGreen assay

DNA coated on the HD-MAP were eluted following repeated (25 times) pipetting of a total volume of 200 μL of ultrapure water (ThermoFisher Scientific) onto the vaccine-coated surface of the patch previously placed in 24-well flat-bottom plates (Thermofisher Scientific). The patch was then flipped in order for the vaccine-coated surface to be fully immersed in the 200 μL of water of each well. The plates were then shaken at speed setting 6 using a titer plate shaker (ThermoFisher Scientific) for 30 min at RT to complete the elution. Eluted DNA and the PicoGreen assay kit dsDNA standard (ThermoFisher Scientific) were serially diluted using 1x TE buffer in a 96-well flat black-bottom plate (Sigma). An equal volume of PicoGreen working solution was added to each well on the plate comprising the serially diluted sample. Plates were left for 5 min at RT and read at an absorbance of 485 nm using the Varioskan Plate Reader (Thermofisher Scientific).

Virus challenge and viral load analysis

Immunized mice were challenged intravenously with 200 PFU of ZIKV-PRVABC59 and viral loads were analyzed following isolation of viral RNA from the plasma of challenged mice, as we have previously described.[19] In brief, plasma viral RNA was isolated using QIAcube HT (Qiagen, Germany) according to the manufacturer's protocol using IndiSpin QIAcube HT Pathogen Kit (Indical, Germany) and cDNA was synthesized with SuperScript IV VILO Master Mix (ThermoFisher Scientific) after gDNA removal step. Viral loads were quantified using an FAM-probe-based RT-qPCR specific for ZIKV capsid as previously described.[19]

Serum and vaginal lavage sample preparation for analysis

Blood was collected via the tail vein using ∼1-mm incision of the tip of the mouse tail or via cardiac puncture in live or euthanized mice, respectively. Blood samples were stored at 4°C for 6–24 h and spun at 10,000 × *g* for 10 min at 4°C prior to isolation of the sera. Each serum sample was heat-inactivated at 56°C for 30 min and stored at −20°C prior to analysis.

In order to evaluate cervicovaginal immunity, 50 μL of sterile phosphate buffered saline (PBS) was pipetted up and down the vaginal lumen three times prior to depositing the PBS representing the vaginal lavage into Eppendorf tubes placed in wet ice. The vaginal lavage samples were spun at 500 × *g* for 5 min at 4°C to pellet and discard the cells. The supernatant was stored at −20°C prior to analysis.

ELISA

Serum and cervicovaginal lavage sample ELISAs were performed adapting the methodology we have previously described to determine anti-NS1 endpoint titer.[19] In brief, Nunc MaxiSorp 96-well flat-bottom plates were coated with 50 μL/well of 1 μg/mL of ZIKV NS1 protein (Sino Biological) in PBS for 16–20 h at 4°C. The plates were washed with 150 μL/well of PBS +0.05% Tween four times prior to pat-drying the plates and incubating the plates with 50 μL/well of StartingBlock Block Buffer (Thermofisher Scientific) for 5 min at RT. Serum or cervicovaginal lavage samples serially diluted using the Block Buffer were added to the plates at 50 μL/well for 1 h at 37°C prior to washing the plates thrice with PBS +0.05% Tween. The plates were then pat-dried to facilitate addition of 50 μL/well of horseradish peroxidase (HRP) conjugated anti-mouse IgG or IgA secondary antibodies (Invitrogen) at 1:3,000 dilution. Following 1 h of incubation at 37°C with HRP-conjugated antibodies, the plates were washed as before and pat-dried. Fifty microliters of 1-Step Ultra TMB-ELISA Substrate Solution (Thermofisher Scientific) was added to each well for 1–3 min at RT prior to addition of 50 μL/well 2M H_2SO_4. The plates were then read immediately at an absorbance of 450 nm using the CLARIOstar Plus microplate reader (BMG LABTECH). Endpoint titers were determined as the reciprocal of the highest serum sample dilution with an optical density reading above the cutoff, set as two standard deviations above the mean optical density of serum samples from pVAX-vaccinated mice.

FTA analysis

The FTA used to measure T cell responses *in vivo* was generated using established protocols described previously.[41,42] Combination of two cell tracking dyes, CTV (Invitrogen) and CPD (eBioscience), were used to label naive, autologous splenocytes prior to pulsing with peptides or peptide pools spanning the NS1 protein. In brief, splenocytes from 12 naive BALB/c mice were pooled, split evenly across five tubes and labeled with either 84.8, 22.95, 6.21, 1.67, or 0.595 μM CTV for 5 min at RT prior to washing the cells thrice. The cells from each CTV-labeled tube were split evenly two ways and labeled with either 9.89 or 38.65 μM CPD prior to performing the three washes again. Just prior to all labeling procedures, splenocytes from each tube were resuspended in 1.9 mL of Roswell Park Memorial Institute 1640 (RPMI, GIBCO) media supplemented with 10% heat-inactivated fetal bovine serum

(HI-FBS), 25 mM (N-2-hydroxyenthylpiperazine-N-2-ethane sulfonic acid (HEPES, GIBCO), 1x 2-mercaptoethanol (GIBCO), 1 mM Sodium Pyruvate (GIBCO), and 50 U/mL of Penicillin-Streptomycin (GIBCO). Cells were washed using the same media and supplements, but the HI-FBS was used at 5%.

Labeled cells were pulsed with mock (nil) or 10 μg/mL of the indicated peptides or peptide pools for 4 h at 37°C + 5% CO_2. NS1 peptide array (PRVABC59, NR-50534) was obtained from the BEI Resources, the National Institute of Allergy and Infectious Diseases and the National Institutes of Health. The array comprise of individual peptides that are 13- or 15-mers in length with 12-amino acid overlap (www.beiresources.org/Catalog/BEIPeptideArrays/NR-50534.aspx).

Following peptide pulsing, the cells were washed and resuspended in PBS (pH 7.4) at a density that allowed intravenous injection of 2 million target cells per fluorescent bar-coded population into immunized mice. Splenocytes from FTA-challenged mice were harvested 18 h after injection, depleted of red blood cells, and stained with 1:400 diluted BUV737 conjugated anti-mouse B220 and 1:100 diluted phycoerythrin-Cyanine 7 (BD Biosciences) conjugated anti-mouse CD69 (BD Biosciences). Stained samples were analyzed using the BD LSR II flow cytometer and data were analyzed using FlowJo 10.8.1 software.

The reduction in the percentage recovery of FTA targets pulsed with cognate NS1 peptides relative to the mock pulsed cells indicate the magnitude of the killing response of CTL. The up-regulation levels of the activation marker, CD69, on naive B cells ($B220^+$) in the FTA presenting cognate peptides to $CD4^+$ Th cells indicate the magnitude of the Th cell-mediated costimulatory response required to activate naive B cells.[32,41] Average responses to the mock pulsed target populations were used to establish the background response for each FTA-challenged mouse and to subtract the responses from the peptide-pulsed targets. To delineate the most robust T cell responses elicited following pVAX-tpaNS1 vaccination stringently, the highest response for each peptide-pulsed target population in the placebo (pVAX) vaccinated group was used to set the highest possible background value and to subtract from the peptide-pulsed target cell responses in pVAX-tpaNS1 vaccinated mice.

Graphs, diagrams, and statistical analysis

Graphs were constructed using GraphPad Prism version 9.0 and p values were calculated using Prism or IBM SPSS statistical analysis software as described in Mekonnen et al.[32] and Grubor-Bauk et al.[19] Diagrams for the study schedules and graphical abstract were constructed using BioRender.

DATA AND CODE AVAILABILITY

Data generated from the current study can be made available upon reasonable request from the corresponding authors.

SUPPLEMENTAL INFORMATION

Supplemental information can be found online at https://doi.org/10.1016/j.omtn.2023.102056.

ACKNOWLEDGMENTS

The Advanced Queensland Industry Research Fellowship funding awarded to D.A.M. and The Hospital Research Foundation Group Fellowship funding awarded to Branka Grubor-Bauk supported the study. We are grateful for the flow cytometry support of Virginia Nink and the Queensland Brain Institute's flow cytometry facility.

AUTHOR CONTRIBUTIONS

D.K.W., D.A.M., and B.G. conceived the study and wrote the initial drafts of the manuscript. A.Y. performed and analyzed data associated with live virus challenge, ELISA, immunofluorescence, and vaccine batch preparation experiments. C.D.M. and J.J.Y.C. optimized vaccine delivery into the skin using the HD-MAP and C.D.M. supervised A.T. during the vaccine stability analysis. A.T. and Z.A.M. performed and analyzed data for the vaccine stability analysis. M.G.M. performed and analyzed ELISA data for cervicovaginal lavage samples. D.K.W. performed and analyzed the FTA experiment. E.J.G. and P.R.Y. reviewed, edited, and provided valuable feedback to finalize the manuscript for submission. All authors have reviewed and approve the manuscript for submission.

DECLARATION OF INTERESTS

The authors declare no competing interests.

REFERENCES

1. Gubler, D.J., Vasilakis, N., and Musso, D. (2017). History and Emergence of Zika Virus. J. Infect. Dis. *216*, S860–S867. https://doi.org/10.1093/infdis/jix451.
2. Regla-Nava, J.A., Wang, Y.T., Fontes-Garfias, C.R., Liu, Y., Syed, T., Susantono, M., Gonzalez, A., Viramontes, K.M., Verma, S.K., Kim, K., et al. (2022). A Zika virus mutation enhances transmission potential and confers escape from protective dengue virus immunity. Cell Rep. *39*, 110655. https://doi.org/10.1016/j.celrep.2022.110655.
3. Maxian, O., Neufeld, A., Talis, E.J., Childs, L.M., and Blackwood, J.C. (2017). Zika virus dynamics: When does sexual transmission matter? Epidemics *21*, 48–55. https://doi.org/10.1016/j.epidem.2017.06.003.
4. Moreira, J., Peixoto, T.M., Siqueira, A.M., and Lamas, C.C. (2017). Sexually acquired Zika virus: a systematic review. Clin. Microbiol. Infect. *23*, 296–305. https://doi.org/10.1016/j.cmi.2016.12.027.
5. Brasil, P., Pereira, J.P., Jr., Moreira, M.E., Ribeiro Nogueira, R.M., Damasceno, L., Wakimoto, M., Rabello, R.S., Valderramos, S.G., Halai, U.A., Salles, T.S., et al. (2016). Zika Virus Infection in Pregnant Women in Rio de Janeiro. N. Engl. J. Med. *375*, 2321–2334. https://doi.org/10.1056/NEJMoa1602412.
6. Pierson, T.C., and Diamond, M.S. (2018). The emergence of Zika virus and its new clinical syndromes. Nature *560*, 573–581. https://doi.org/10.1038/s41586-018-0446-y.
7. Pattnaik, A., Sahoo, B.R., and Pattnaik, A.K. (2020). Current status of Zika virus vaccines: successes and challenges. Vaccines *8*. https://doi.org/10.3390/vaccines8020266.
8. Dejnirattisai, W., Supasa, P., Wongwiwat, W., Rouvinski, A., Barba-Spaeth, G., Duangchinda, T., Sakuntabhai, A., Cao-Lormeau, V.M., Malasit, P., Rey, F.A., et al. (2016). Dengue virus sero-cross-reactivity drives antibody-dependent enhancement of infection with zika virus. Nat. Immunol. *17*, 1102–1108. https://doi.org/10.1038/ni.3515.
9. Stettler, K., Beltramello, M., Espinosa, D.A., Graham, V., Cassotta, A., Bianchi, S., Vanzetta, F., Minola, A., Jaconi, S., Mele, F., et al. (2016). Specificity, cross-reactivity, and function of antibodies elicited by Zika virus infection. Science *353*, 823–826. https://doi.org/10.1126/science.aaf8505.
10. Kawiecki, A.B., and Christofferson, R.C. (2016). Zika Virus-Induced Antibody Response Enhances Dengue Virus Serotype 2 Replication In Vitro. J. Infect. Dis. *214*, 1357–1360. https://doi.org/10.1093/infdis/jiw377.
11. Bailey, M.J., Duehr, J., Dulin, H., Broecker, F., Brown, J.A., Arumemi, F.O., Bermúdez González, M.C., Leyva-Grado, V.H., Evans, M.J., Simon, V., et al. (2018). Human

antibodies targeting Zika virus NS1 provide protection against disease in a mouse model. Nat. Commun. *9*, 4560. https://doi.org/10.1038/s41467-018-07008-0.

12. Xu, X., Vaughan, K., Weiskopf, D., Grifoni, A., Diamond, M.S., Sette, A., and Peters, B. (2016). Identifying Candidate Targets of Immune Responses in Zika Virus Based on Homology to Epitopes in Other Flavivirus Species. PLoS Curr. *8*. https://doi.org/10.1371/currents.outbreaks.9aa2e1fb61b0f632f58a098773008c4b.
13. Muller, D.A., and Young, P.R. (2013). The flavivirus NS1 protein: molecular and structural biology, immunology, role in pathogenesis and application as a diagnostic biomarker. Antivir. Res. *98*, 192–208. https://doi.org/10.1016/j.antiviral.2013.03.008.
14. Jorritsma, S.H.T., Gowans, E.J., Grubor-Bauk, B., and Wijesundara, D.K. (2016). Delivery methods to increase cellular uptake and immunogenicity of DNA vaccines. Vaccine *34*, 5488–5494. https://doi.org/10.1016/j.vaccine.2016.09.062.
15. Kim, T.J., Jin, H.T., Hur, S.Y., Yang, H.G., Seo, Y.B., Hong, S.R., Lee, C.W., Kim, S., Woo, J.W., Park, K.S., et al. (2014). Clearance of persistent HPV infection and cervical lesion by therapeutic DNA vaccine in CIN3 patients. Nat. Commun. *5*, 5317. https://doi.org/10.1038/ncomms6317.
16. Trimble, C.L., Morrow, M.P., Kraynyak, K.A., Shen, X., Dallas, M., Yan, J., Edwards, L., Parker, R.L., Denny, L., Giffear, M., et al. (2015). Safety, efficacy, and immunogenicity of VGX-3100, a therapeutic synthetic DNA vaccine targeting human papillomavirus 16 and 18 E6 and E7 proteins for cervical intraepithelial neoplasia 2/3: a randomised, double-blind, placebo-controlled phase 2b trial. Lancet *386*, 2078–2088. https://doi.org/10.1016/S0140-6736(15)00239-1.
17. Larocca, R.A., Abbink, P., Peron, J.P.S., Zanotto, P.M.d.A., Iampietro, M.J., Badamchi-Zadeh, A., Boyd, M., Ng'ang'a, D., Kirilova, M., Nityanandam, R., et al. (2016). Vaccine protection against Zika virus from Brazil. Nature *536*, 474–478. https://doi.org/10.1038/nature18952.
18. Abbink, P., Larocca, R.A., De La Barrera, R.A., Bricault, C.A., Moseley, E.T., Boyd, M., Kirilova, M., Li, Z., Ng'ang'a, D., Nanayakkara, O., et al. (2016). Protective efficacy of multiple vaccine platforms against Zika virus challenge in rhesus monkeys. Science *353*, 1129–1132. https://doi.org/10.1126/science.aah6157.
19. Grubor-Bauk, B., Wijesundara, D.K., Masavuli, M., Abbink, P., Peterson, R.L., Prow, N.A., Larocca, R.A., Mekonnen, Z.A., Shrestha, A., Eyre, N.S., et al. (2019). NS1 DNA vaccination protects against Zika infection through T cell-mediated immunity in immunocompetent mice. Sci. Adv. *5*, eaax2388. https://doi.org/10.1126/sciadv.aax2388.
20. Roth, G.A., Picece, V.C.T.M., Ou, B.S., Luo, W., Pulendran, B., and Appel, E.A. (2022). Designing spatial and temporal control of vaccine responses. Nat. Rev. Mater. *7*, 174–195. https://doi.org/10.1038/s41578-021-00372-2.
21. Fernando, G.J.P., Chen, X., Prow, T.W., Crichton, M.L., Fairmaid, E.J., Roberts, M.S., Frazer, I.H., Brown, L.E., and Kendall, M.A.F. (2010). Potent immunity to low doses of influenza vaccine by probabilistic guided micro-targeted skin delivery in a mouse model. PLoS One *5*, e10266. https://doi.org/10.1371/journal.pone.0010266.
22. Fernando, G.J.P., Hickling, J., Jayashi Flores, C.M., Griffin, P., Anderson, C.D., Skinner, S.R., Davies, C., Witham, K., Pryor, M., Bodle, J., et al. (2018). Safety, tolerability, acceptability and immunogenicity of an influenza vaccine delivered to human skin by a novel high-density microprojection array patch (Nanopatch). Vaccine *36*, 3779–3788. https://doi.org/10.1016/j.vaccine.2018.05.053.
23. Depelsenaire, A.C.I., Witham, K., Veitch, M., Wells, J.W., Anderson, C.D., Lickliter, J.D., Rockman, S., Bodle, J., Treasure, P., Hickling, J., et al. (2021). Cellular responses at the application site of a high-density microarray patch delivering an influenza vaccine in a randomized, controlled phase I clinical trial. PLoS One *16*, e0255282. https://doi.org/10.1371/journal.pone.0255282.
24. Elong Ngono, A., Syed, T., Nguyen, A.V., Regla-Nava, J.A., Susantono, M., Spasova, D., Aguilar, A., West, M., Sparks, J., Gonzalez, A., et al. (2020). CD8(+) T cells mediate protection against Zika virus induced by an NS3-based vaccine. Sci. Adv. *6*, eabb2154. https://doi.org/10.1126/sciadv.abb2154.
25. Gambino, F., Jr., Tai, W., Voronin, D., Zhang, Y., Zhang, X., Shi, J., Wang, X., Wang, N., Du, L., and Qiao, L. (2021). A vaccine inducing solely cytotoxic T lymphocytes fully prevents Zika virus infection and fetal damage. Cell Rep. *35*, 109107. https://doi.org/10.1016/j.celrep.2021.109107.
26. Lima, N.S., Rolland, M., Modjarrad, K., and Trautmann, L. (2017). T Cell Immunity and Zika Virus Vaccine Development. Trends Immunol. *38*, 594–605. https://doi.org/10.1016/j.it.2017.05.004.
27. Grifoni, A., Pham, J., Sidney, J., O'Rourke, P.H., Paul, S., Peters, B., Martini, S.R., de Silva, A.D., Ricciardi, M.J., Magnani, D.M., et al. (2017). Prior Dengue Virus Exposure Shapes T Cell Immunity to Zika Virus in Humans. J. Virol. *91*, e01469-17. https://doi.org/10.1128/JVI.01469-17.
28. Song, H., Qi, J., Haywood, J., Shi, Y., and Gao, G.F. (2016). Zika virus NS1 structure reveals diversity of electrostatic surfaces among flaviviruses. Nat. Struct. Mol. Biol. *23*, 456–458. https://doi.org/10.1038/nsmb.3213.
29. Modhiran, N., Song, H., Liu, L., Bletchly, C., Brillault, L., Amarilla, A.A., Xu, X., Qi, J., Chai, Y., Cheung, S.T.M., et al. (2021). A broadly protective antibody that targets the flavivirus NS1 protein. Science *371*, 190–194. https://doi.org/10.1126/science.abb9425.
30. Biering, S.B., Akey, D.L., Wong, M.P., Brown, W.C., Lo, N.T.N., Puerta-Guardo, H., Tramontini Gomes de Sousa, F., Wang, C., Konwerski, J.R., Espinosa, D.A., et al. (2021). Structural basis for antibody inhibition of flavivirus NS1-triggered endothelial dysfunction. Science *371*, 194–200. https://doi.org/10.1126/science.abc0476.
31. Wessel, A.W., Kose, N., Bombardi, R.G., Roy, V., Chantima, W., Mongkolsapaya, J., Edeling, M.A., Nelson, C.A., Bosch, I., Alter, G., et al. (2020). Antibodies targeting epitopes on the cell-surface form of NS1 protect against Zika virus infection during pregnancy. Nat. Commun. *11*, 5278. https://doi.org/10.1038/s41467-020-19096-y.
32. Mekonnen, Z.A., Grubor-Bauk, B., English, K., Leung, P., Masavuli, M.G., Shrestha, A.C., Bertolino, P., Bowen, D.G., Lloyd, A.R., Gowans, E.J., and Wijesundara, D.K. (2019). Single-Dose Vaccination with a Hepatotropic Adeno-associated Virus Efficiently Localizes T Cell Immunity in the Liver with the Potential To Confer Rapid Protection against Hepatitis C Virus. J. Virol. *93*, e00202-19. https://doi.org/10.1128/JVI.00202-19.
33. Beaver, J.T., Mills, L.K., Swieboda, D., Lelutiu, N., Esser, E.S., Antao, O.Q., Scountzou, E., Williams, D.T., Papaioannou, N., Littauer, E.Q., et al. (2020). Cutaneous vaccination ameliorates Zika virus-induced neuro-ocular pathology via reduction of anti-ganglioside antibodies. Hum. Vaccines Immunother. *16*, 2072–2091. https://doi.org/10.1080/21645515.2020.1775460.
34. Zhang, H., Xiao, W., Zhao, M., Zhao, Y., Zhang, Y., Lu, D., Lu, S., Zhang, Q., Peng, W., Shu, L., et al. (2022). The CD8+ and CD4+ T Cell Immunogen Atlas of Zika Virus Reveals E, NS1 and NS4 Proteins as the Vaccine Targets. Viruses *14*. https://doi.org/10.3390/v14112332.
35. Takeuchi, A., Badr, M.E.S.G., Miyauchi, K., Ishihara, C., Onishi, R., Guo, Z., Sasaki, Y., Ike, H., Takumi, A., Tsuji, N.M., et al. (2016). CRTAM determines the CD4+ cytotoxic T lymphocyte lineage. J. Exp. Med. *213*, 123–138. https://doi.org/10.1084/jem.20150519.
36. Takeuchi, A., and Saito, T. (2017). CD4 CTL, a Cytotoxic Subset of CD4(+) T Cells, Their Differentiation and Function. Front. Immunol. *8*, 194. https://doi.org/10.3389/fimmu.2017.00194.
37. Klinman, D.M., Yamshchikov, G., and Ishigatsubo, Y. (1997). Contribution of CpG motifs to the immunogenicity of DNA vaccines. J. Immunol. *158*, 3635–3639.
38. Pulendran, B., S Arunachalam, P., and O'Hagan, D.T. (2021). Emerging concepts in the science of vaccine adjuvants. Nat. Rev. Drug Discov. *20*, 454–475. https://doi.org/10.1038/s41573-021-00163-y.
39. McMillan, C.L.D., Choo, J.J.Y., Idris, A., Supramaniam, A., Modhiran, N., Amarilla, A.A., Isaacs, A., Cheung, S.T.M., Liang, B., Bielefeldt-Ohmann, H., et al. (2021). Complete protection by a single-dose skin patch-delivered SARS-CoV-2 spike vaccine. Sci. Adv. *7*, eabj8065. https://doi.org/10.1126/sciadv.abj8065.
40. Choo, J.J.Y., Vet, L.J., McMillan, C.L.D., Harrison, J.J., Scott, C.A.P., Depelsenaire, A.C.I., Fernando, G.J.P., Watterson, D., Hall, R.A., Young, P.R., et al. (2021). A chimeric dengue virus vaccine candidate delivered by high density microarray patches protects against infection in mice. NPJ Vaccines *6*, 66. https://doi.org/10.1038/s41541-021-00328-1.
41. Quah, B.J.C., Wijesundara, D.K., Ranasinghe, C., and Parish, C.R. (2012). Fluorescent target array killing assay: a multiplex cytotoxic T-cell assay to measure detailed T-cell antigen specificity and avidity in vivo. Cytometry A. *81*, 679–690. https://doi.org/10.1002/cyto.a.22084.
42. Wijesundara, D.K., Ranasinghe, C., Jackson, R.J., Lidbury, B.A., Parish, C.R., and Quah, B.J.C. (2014). Use of an in vivo FTA assay to assess the magnitude, functional avidity and epitope variant cross-reactivity of T cell responses following HIV-1 recombinant poxvirus vaccination. PLoS One *9*, e105366. https://doi.org/10.1371/journal.pone.0105366.